Optimal separation of the coseismic and postseismic deformation from the tectonic motion

(Progress Report)

Danan Dong
Space Geodetic Science and Applications Group
Jet Propulsion Laboratory, California Institute of Technology, Pasadena, California

1. INTRODUCTION

In the last two years, several research groups revisited the postseismic deformation of the 1992 Landers earthquake from GPS measurements (Bock et al., 1997; Savage & Svarc., 1997) and SAR measurements (Massonnet et al., 1996; Peltzer et al., 1996). The new data reveal the long term postseismic deformation mode besides the short term transient postseismic deformation mode (Shen et al., 1994). The nature of the postseismic deformation, however, remains controversial due to poor data coverage (short span, narrow aperture, few sites, etc.). In particular, the vertical measurements turn out to be critical for exploring the nature of the postseismic deformation (Deng et al., 1998) as well as for reconciling the discrepancy between GPS and SAR results. SCEC archived GPS southern California campaign data provide more complete coverage and span about the postseismic deformation of the Landers earthquake. I revisit these GPS campaign data and try to optimally extract the postseismic deformation using the technique imbedded in the QOCA software (see web page http://sideshow.jpl.nasa.gov/~dong/qoca for details). I report my preliminary results here.

2. STRATEGY OF EXTRACTING THE POSTSEISMIC DEFORMATION

The SCEC archived GPS southern California campaign data were processed using GAMIT software. All raw solutions were loosely constrained daily solutions. Then these daily solutions were combined by GLOBK software to form loosely constrained campaign solutions. Keep loose constraining is necessary and important to maintain an uniform reference frame for all the campaign solutions. These loosely constrained campaign solutions were used by QOCA software as the quasi-observations for further combination to get the tectonic information. The general combination strategy is described in Dong et al. (1998) and will not be repeated here. In this analysis, however, there were four unique strategies which should be reported here.

1). The GAMIT routine process leaves several systematic terms uncorrected. Among these terms, the most significant are pole tide correction, ocean tide correction and atmospheric loading correction. Quantitative assessment (my another project work, which will not be reported here) indicates that these systematic terms are significant, which could reach several centimeters in vertical and 1/3 of vertical displacements in horizontal. In my analysis, I used the IERS formula to perform the pole tide correction. The ocean tide loading caused site displacements were calculated using the coefficients provided by Dr. Scherneck. For the campaign quasi-observations, the information of high frequency site displacements was lost. So that I did not perform the diurnal and semidiurnal ocean tide loading corrections. Only Mf, Mm, and Ssa tide loading corrections were implemented. Scherneck's coefficients did not include the Sa tide so that I did not perform the Sa tide correction. It unlikely caused serious problem because the amplitude of the Sa tidal force is one order smaller that that of Ssa and the vertical site displacements due to Sa tide are expected to be at the mm level or less. NCEP reanalysis surface pressure data (6-hr sampling) were used to calculate the atmospheric loading effects. 18 years (from 1980 to

1997) averaged surface grid pressure data were used to calculate the pressure variations from the average. Global Green function convolution approach was adopted and Farrell's program was utilized. Due to the manpower limit, the groundwater and non-tidal sea surface variation caused site displacements were not calculated yet. They will be implemented soon.

2). Since the coverage of the global tracking stations and the constellation of GPS satellites were much improved after the Landers earthquake, I adopted the internal constraint approach (see Appendix C of Dong et al., 1998) to define the reference frame. Based on the coverage of the GPS campaign quasi-observations, I selected the following 16 site to form the internal constraints: VNDP, GOLD, ALBH, PIE1, ONSA, WTZ1, KOSG, TROM, FAIR, DRAO, STJO, HERS, MADR, KOKB, ALGO, YELL. Such a selection was probably not optimal for the study of global tectonics, but was adequate to define an uniform reference frame for the region affected by the Landers postseismic deformation. Among the 16 sites, only GOLD was affected by the postseismic deformation. The consistency of the remaining 15 unaffected sites seems pretty good so that the time series at GOLD still show clear postseismic deformation which is consistent with the results of Bock et al. (1997). 7-parameter transformation were used (3 network rotations, 3 network translations, 1 scaling factor) for the internal constraints.

3). I used the separate mode (estimate individual solutions separately for campaign data) and dejump option (remove apriori velocities and coseismic displacements from the time series) to get the time series for each site, which contain mostly the postseismic deformation information.

4). For the position time series of each site, I estimated the bias, amplitude and relaxation characteristic time parameters for the horizontal components (5 parameters for each E-N pair). For the short span (1992-1998), the difference between the exponential decay curve and the logarithmic relaxation curves are nearly not distinguishable for the far-field sites, but the near-field sites are prefer to the logarithmic model so that I used the logarithmic model. SCEC velocity map version 2.0 solutions (with slight modification) were used as the default velocity field. The correlation between east and north position components was taken into account. The characteristic time for east and north components was constrained to be the same. Iteration approach was implemented. Although I did not use the full covariance matrix, such a strategy gave me more flexibility to monitor the position variations of each site and to prevent some abnormal behaviors at several sites from contaminating solutions at the other sites.

3. POSTSEISMIC DEFORMATION FIELD

Among the sites GPS campaign occupied, there were 65 sites with multiple observations (more than 3) and spanning more than 2 years after the Landers earthquake. The adjusted characteristic times (τ) were 0.9 - 1.7 years with the average of 1.35 years, which is slightly larger than the estimate of 1.215 year of Savage and Svarc (1997), probably due to different space and span coverage. Since the estimated τ were fairly close, the mechanism which generated the postseismic deformation could be described by a single model to the first degree approximation. The spatial distribution of the postseismic deformation field is shown in Figure 1. Where the arrows represent the estimated amplitudes and the ellipses represent the 1-σ errors. The major features of Figure 1 are: (1) The postseismic deformation field is similar to the coseismic deformation field but with smaller amplitude contrast, indicating similar fault dislocation plane with deeper depth; (2) The largest amplitudes are at the southern part of the rupture fault segments; (3) The magnitudes of the postseismic deformation field at the near-field sites are in good agreement with the modified Savage (1997) model (there are some gaps between the fault segments of the original Savage model, we modify his model by fitting the gaps). But there are some discrepancies of the orientations of our postseismic deformation field with that of Savage model. The details of the geophysical explanation and our inverse result of the postseismic fault slip distribution are my another project and will not be reported here.

The derived vertical postseismic deformation field is more complicated than the horizontal postseismic deformation field. Data noise is one of the reasons which cause the irregularities of the vertical position variations at far-field sites. Multiple vertical deformation mechanisms are the plausible reasons too. The quality of the GPS derived vertical site positions seems not as bad as we previously thought. In particular, the time series of the vertical positions at the near-field sites show clear exponential decay curves, which provide important constraints for exploring the postseismic deformation mechanisms. We will finish the final combination and construct our inverse model in this year (1999).

REFERENCES

Bock, Y., et al., Southern California Permanent GPS Geodetic Array: continuous measurements of regional crustal deformation between the 1992 Landers and 1994 Northridge earthquakes, *J. Geophys. Res*., 102, 18013-18033, 1997

Dong, D., T. H. Herring, and R. W. King, Estimating regional deformation from a combination of Space and terrestrial geodetic data, in press, *Journal of Geodesy*, 1997

Deng, J. C., et al. Viscoelastic flow in the lower crust after the 1992 Landers, California, earthquake, *Science*, 282, 1689-1692, 1998

Massonnet, D., et al. Radar interferometry detects two mechanisms of postseismic relaxation following the Landers California earthquake, *Nature*, 382612-616, 1996

Peltzer, G., et al. Postseismic rebound in fault step-overs caused by pore fluid flow, *Science*, 273, 1202-1204, 1996

Savage, J. C. and J. L. Svarc, Postseismic deformation associated with the 1992 M_w = 7.3 Landers earthquake, Southern California, *J. Geophys. Res*., 102, 7565-7577, 1997

Shen, Z., et al., Postseismic deformation following the Landers earthquake, Calif., June 28, 1992, *Bull*. Seis. Soc. Amer., 84, 780-791, 1994

Figure 1. Postseismic deformation field (horizontal) from Landers earthquake

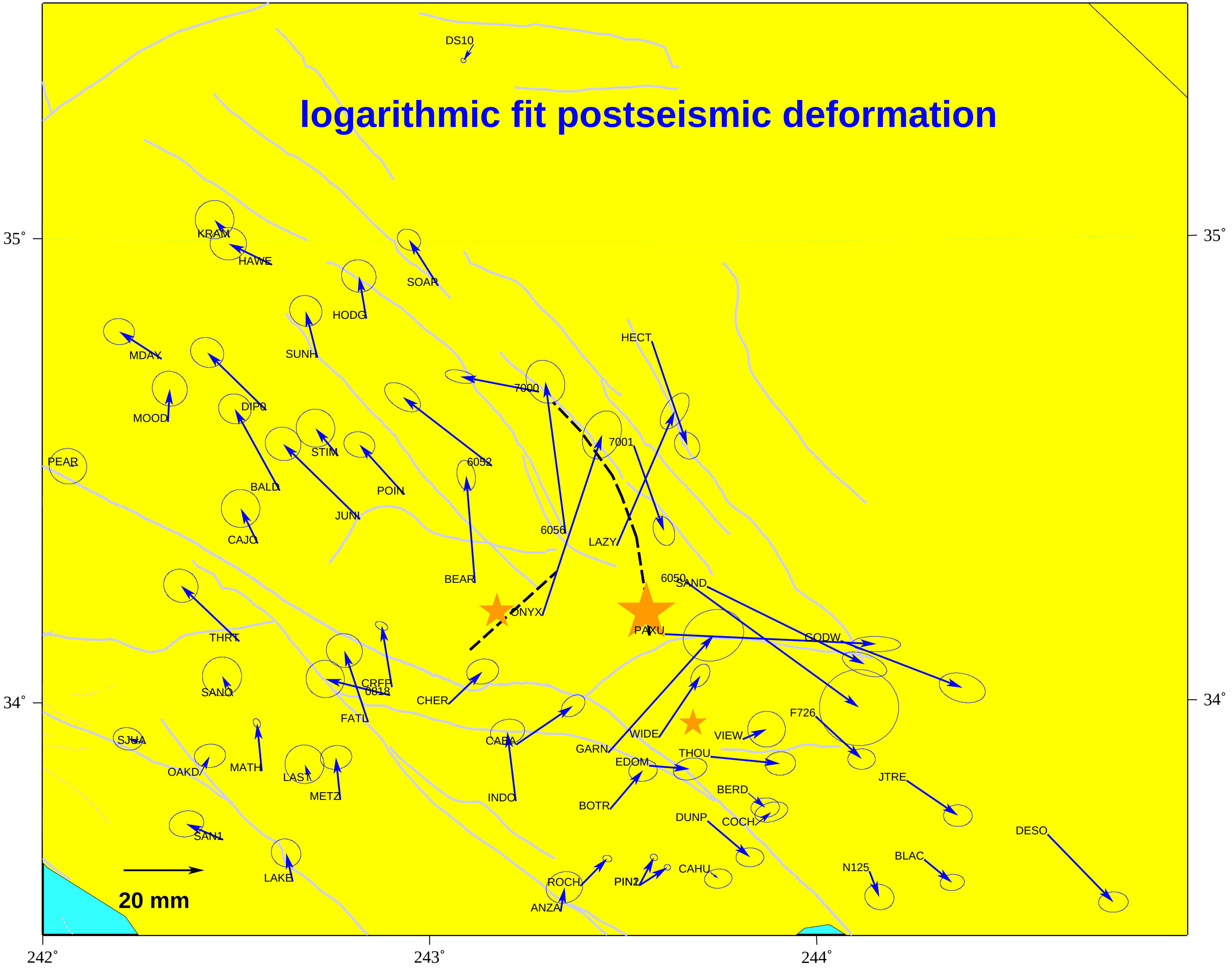

logarithmic fit postseismic deformation